



Published in final edited form as:

*Clin Cancer Res.* 2015 October 15; 21(20): 4619–4629. doi:10.1158/1078-0432.CCR-15-0242.

## Notch pathway inhibition using PF-03084014, a $\gamma$ -secretase inhibitor (GSI), enhances the anti-tumor effect of docetaxel in prostate cancer

Di Cui<sup>1,2</sup>, Jinlu Dai<sup>1</sup>, Jill M. Keller<sup>1,3</sup>, Atsushi Mizokami<sup>4</sup>, Shujie Xia<sup>2</sup>, and Evan T. Keller<sup>1,5</sup>

<sup>1</sup>Department of Urology, University of Michigan, Ann Arbor, MI USA

<sup>2</sup>Department of Urology, Shanghai First People's Hospital, School of Medicine, Shanghai Jiao Tong University, Shanghai, China

<sup>3</sup>Unit for Laboratory Animal Medicine, University of Michigan, Ann Arbor MI USA

<sup>4</sup>Department of Urology, Kanazawa University, Kanazawa, Japan

<sup>5</sup>Biointerfaces Institute, University of Michigan, Ann Arbor, MI USA

### Abstract

**Purpose**—To investigate the efficacy and mechanisms of Notch signaling inhibition as an adjuvant to docetaxel in castration-resistant prostate cancer (CRPC) using a  $\gamma$ -secretase inhibitor (GSI), PF-03084014.

**Experimental Design**—The effect of PF-03084014 on response to docetaxel was evaluated in docetaxel-sensitive and -resistant CRPC cell lines *in vitro* and in murine models. Both soft tissue and bone sites were evaluated *in vivo*. Impacts on cell proliferation, apoptosis, cancer stem cells and angiogenesis were evaluated.

**Results**—The combination of PF-03084014 plus docetaxel reduced both docetaxel-sensitive and -resistant CRPC tumor growth in soft tissue and bone greater than either agent alone. Antitumor activity was associated with PF-03084014-induced inhibition of Notch pathway signaling; decreased survival signals (Cyclin E; MEK-ERK, PI3K-AKT, EGFR and NF- $\kappa$ B pathway; BCL-2, BCL-XL); increased apoptotic signals (BAK, BAX; cleaved-caspase 3); reduction of microvessel density; reduced epithelial mesenchymal transition; and reduction of cancer stem-like cells in the tumor.

**Conclusion**—These results reveal that PF-03084014 enhances docetaxel-mediated tumor response and provides a rationale to explore GSIs as adjunct therapy in conjunction with docetaxel for men with CRPC.

### Keywords

Prostate cancer;  $\gamma$ -secretase inhibitor; Notch; docetaxel resistance; bone metastasis

Corresponding authors: Evan T. Keller DVM, PhD Department of Urology, RM 5308 CCGC, University of Michigan, Ann Arbor, MI 48109-8940, USA Tel.: 734-615-0280. etkeller@umich.edu; Shujie Xia, MD, PhD Department of Urology, Shanghai First People's Hospital, 100 Haining Road, Shanghai 200080, China. Tel.: 86-21-63240090-3161. xsjurologist@163.com.

Conflicts of interest: ET Keller received research funding from Pfizer for the studies in this report.

## Introduction

Prostate cancer remains a major health problem, as it is the most common cancer in adult males and second cause of cancer death in most western countries. It is estimated that in 2013, 240 thousand American men were diagnosed and nearly 30 thousand died of the disease (1). Most prostate cancer deaths are associated with the development of castration-resistant prostate cancer (CRPC) (2). When androgen deprivation therapy fails and CRPC develops, docetaxel is frequently utilized as a first line chemotherapy and has shown a survival advantage (3). However, not all the patients respond to docetaxel (4) and in those that do, docetaxel resistance eventually develops. Second generation taxanes, such as cabazitaxel, have been shown to be effective in some cases of docetaxel resistance; however, those patients eventually fail cabazitaxel (5). Accordingly, developing adjuvant therapies that enhance taxane activity could provide a major benefit to patients.

The Notch pathway is a conserved signaling pathway that contributes to cell fate determination, proliferation, angiogenesis and apoptosis. It has been recently identified that the Notch pathway is not a simple linear sequence of events, as it can crosstalk with other signaling pathways to form an extraordinarily complex network (6, 7). Abnormalities in the Notch pathway have been reported to play roles in prostate development and potentially prostate cancer progression (8-10). Gene array analysis of clinical samples demonstrated up-regulation of Notch pathway components in high grade localized disease (10). Targeting the notch pathway ligand Jagged-1 can induce cell growth inhibition and S phase arrest (11); knockdown of Notch 1 receptor can also inhibit prostate cancer cell growth, migration and invasion via inactivation of Akt, mTOR, and NF- $\kappa$ B signaling pathways (12, 13). Taken together, these studies suggest targeting the Notch pathway may provide clinical benefit for prostate cancer patients. Furthermore, it has been identified that a subpopulation of cells that survive docetaxel exposure overexpress Notch and Hedgehog signaling pathways and that targeting these pathways could deplete the docetaxel resistant cells (14). This finding provided us with the rationale to evaluate if pharmacological targeting of the Notch pathway could impact docetaxel chemoresistance in prostate cancer.

PF-03084014, a gamma secretase inhibitor (GSI), has been shown to inhibit Notch pathway signaling through blocking cleaved-notch receptor formation in T-ALL (15), breast cancer (16), pancreatic cancer (17) and colorectal cancer (18). However, the efficacy of PF-03084014 has neither been evaluated in an *in vivo* model of prostate cancer nor in the context of docetaxel resistance. Accordingly, we evaluated the anti-tumor efficacy of PF-03084014 alone and in combination with docetaxel in docetaxel-sensitive and docetaxel-resistant CRPC *in vivo*. We also explored the signaling pathways through which Notch may impact prostate cancer.

## Materials and Methods

### Cell lines and cell culture condition

Human prostate cancer cell lines Du145 and PC3 were obtained from the American Type Culture Collection (ATCC; Rockville, MD) and docetaxel-resistant Du145R and PC3R have

been previously described (19). All the cells were cultured in RPMI 1640 (Invitrogen Co., Carlsbad, CA) supplemented with 10% fetal bovine serum (FBS) and 1% penicillin-streptomycin (Life Technologies, Inc.). Cell identification is completed annually using PCR for short tandem repeats.

### Manipulation of Notch pathway expression

For knockdown studies, cells were transfected with Notch-1 siRNA and siRNA control (Santa Cruz Biotechnology, Santa Cruz, CA) using siRNA Transfection Reagent (Santa Cruz Biotechnology) as recommended by the manufacturer and previously described (20). For overexpression studies, cells were transfected with NICD expression vector (p-CAGGS-NICD) (Addgene, Cambridge, MA) or empty vector using FuGene HD Transfection Reagent (Promega, Madison, WI) as recommended by the manufacturer.

### Cell Viability assay

Du145, PC3 and Du145R, PC3R cells were cultured in 96-well plates for overnight ( $2.5 \times 10^3$  cells/well). Cells were treated with (1) PF-03084014 (0.1  $\mu$ M, 0.5  $\mu$ M, 1  $\mu$ M, 5  $\mu$ M, 10  $\mu$ M; Pfizer) or vehicle (DMSO) for 48hr; (2) Docetaxel (10nM; Cell Signaling Technology) or vehicle (PBS) for 48hr; (3) Docetaxel (0nM, 5nM, 10nM, 25nM, 50nM, 75nM; Cell Signaling Technology) and PF-03084014 (10  $\mu$ M; Pfizer) or vehicle (DMSO) for 48hr. 40  $\mu$ g Resazurin sodium salt (Sigma Aldrich, St Louis, MO) was added into 200  $\mu$ l medium. After two hours incubation, fluorescence was measured with an excitation wavelength of 550 nm and emission 605 nm on a plate reader (Multi-Mode Microplate Reader, SpectraMax M5, Molecular Devices MDS Analytical Technologies).

### Animal studies

7-8 week-old male NOD.CB17-Prkdcscid/NCrCrl (NOD/SCID) mice (Charles River, Wilmington, MA) were housed under pathogen-free conditions. All experimental protocols were approved by the University of Michigan Animal Care and Use Committee. For subcutaneous injection,  $1 \times 10^6$  cells suspensions of Du145, Du145R, PC3 and PC3R cells were injected subcutaneously into the flank. When cohorts of tumors reached 100-200 mm<sup>3</sup>, mice were randomly assigned to control and three treatment groups (10-12 mice per group): (1) vehicle; (2) PF-03084014 (150mg/kg, dissolved in 0.05% Methyl cellulose, daily, p.o., 7-days-on/7-days-off schedule for 4 weeks based on a previous report that indicates this dosage regimen minimizes gastrointestinal toxicity while still maintaining a tumor response (15)); (3) docetaxel (5mg/kg for Du145 and PC3; 10mg/kg for Du145R and PC3R, i.p, weekly for 4 weeks); (4) PF-03084014+docetaxel (same dosage as above for 4 weeks). Tumor size and body weight were measured twice a week. Tumor volume was calculated following the formula: tumor volume  $V = a \times b^2 \times 0.52$ , a length of the tumor, b width of the tumor (17). In the case of the Du145 subcutaneously injected mice (4 groups, 5 mice per group) drug administration was stopped after the 4-week period and the mice were monitored for another 4 weeks to examine for tumor regrowth.

For intratibial injection, after anesthesia and flexing the knee, a 27g 3/8-inch needle was inserted into the proximal end of right tibia followed by injection of 20  $\mu$ l single-cell suspension of Du145R cells ( $2 \times 10^5$  cells). Tumor development in bone was evaluated

weekly using radiography. After 8 weeks, mice were randomly assigned to 4 groups (5 mice per group). Control and treatments were the same as for the subcutaneous groups. Pre- and post-treatment, radiographs was performed and data used to determine tumor growth following the published method (21) .

### **Flow cytometry analysis of alkaline dehydrogenase (ALDH) expression**

Subcutaneous tumors were harvested after 4 weeks of treatment. Single cell suspensions were created using collagenase V. Then ALDH positive cells were evaluated using the ALDEFUOR® assay kit (STEMCELL Technologies, Inc.) according to the manufacturer's protocol. One microgram per milliliter of 7AAD (Sigma-Aldrich, St. Louis, MO) was added to the samples before flow analysis to facilitate dead cell discrimination. Samples were analyzed on BD LSRFortessa™ flow cytometer (BD Biosciences, San Jose, CA).

### **Prostasphere formation**

After 4 weeks treatment, Du145 subcutaneous tumors were made into single cell suspension as described above. One million cells were cultured in ultra-low-attachment 6-well plates (Corning, New York), using serum free DMEM/F12 medium supplemented with 20ng/ml EGF, 20ng/ml bFGF, 5µg/ml insulin and B27 (Invitrogen Co., Carlsbad, CA). After 7 days, the first generation spheres were obtained by filtering medium with 40µM cell strainer (Corning, New York). Trypsin was added to detach cells into single cell suspension. 3000 cells were re-cultured in ultra-low-attachment 48-well plates to form second-generation spheres. The second generation sphere size and numbers were measured using microscopy.

### **Western blot analysis**

Du145 and Du145R subcutaneous xenografts were harvested after treatment and stored at -80°C. Tumor tissues were homogenized in ice-cold RIPA lysis buffer (Millipore, Billerica, MA) containing protease inhibitors and phosphatase inhibitors. The protein concentration of tumor extracts was determined using BCA Protein Assay Kit (Pierce). Target protein expression was analyzed using Western blot analysis, which was done as previously described (22), with β-actin was used as a loading control. Anti-NICD, Cyclin E, BCL-2, BCL-xl, BAK, BAX, MEK1/2, phosphor-MEK1/2( ser217/221), ERK1/2, phosphor-ERK1/2 ( T202/Y204), AKT, phosphor-AKT(ser473), PI3K, phosphor-PI3K(tyr455/199), EGFR, P52, E-cadherin, Snail, Slug, MDR1, NANOG were obtained from Cell Signaling Technology Company (Beverly, MA);β-actin from Sigma Aldrich (St Louis, MO). The antibodies were diluted as recommended by the manufacturers.

### **Quantitative real-time PCR**

Total RNA was extracted from fresh Du145 and Du145R subcutaneous xenografts using RNeasy Mini Kit (Qiagen, Valencia, CA) according to the manufacturer's protocol. Using Superscript III first-strand synthesis system (Invitrogen, Inc.), mRNA was reverse-transcribed into cDNA. SYBR green (Qiagen) were used to amplify cDNA by quantitative real-time reverse transcriptase polymerase chain reaction (qRT-PCR) with the conditions: 1 cycle at 95°C for 10 min, 45 cycles at 95°C for 15 s, 60°C for 60s. The primers were as follows: human HEY1 (forward, 5'-TCTGAGCTGAGAAGGCTGGT-3'; reverse, 5'-

CGAAATCCCAAACACTCCGATA-3'); human HEY2 (forward, 5'-TGAGAAGACTAGTGCCAACAGC-3'; reverse, 5'-TGGGCATCAAAGTAGCCTTTA-3'); human  $\beta$ -actin (forward, 5'-TCATGAAGTGTGACGTTGACATCCGT-3'; reverse, 5'-CCTAGAAGCATTGCGGTGCACGATG-3'). In order to compare the relative expression of mRNA in different samples, the comparative delta Ct (threshold cycle number) was calculated.

### Immunohistochemistry (IHC)

Both tibiae and subcutaneous tumors were fixed in 10% neutral-buffered formalin. Five-micron (5 $\mu$ M) sections were used for H&E and IHC. Ki67 (1:500, Santa Cruz Biotechnology), Cleaved-caspase 3 (1:300, Cell Signaling Biotechnology) and CD31 (1:50, Biocare Medical) were stained as per the manufactures protocols. Sections were examined for positive staining and vessel density that was quantified as previously described (22, 23). Representative fields were photographed under 40 $\times$  magnification.

### Statistical analysis

Numerical data are expressed as mean  $\pm$  SD. Statistical analysis was performed by One-way ANOVA for multiple comparisons, and Student's t-test for bivariate comparisons. Differences with  $P < 0.05$  were determined as statistically significant.

## Results

### PF-03084014 sensitizes docetaxel-resistant cells to docetaxel *in vitro*

To determine if the development of chemoresistance modulated Notch-1 receptor expression we measured its expression in parental docetaxel-sensitive and their daughter docetaxel-resistant cell lines. Notch-1 receptor expression was increased in the docetaxel-resistant variants of the cell line (Fig. 1A). To determine if PF-03084014 impacts the proliferation of CRPC *in vitro*, we evaluated the viability of four cell lines after 48hr of GSI treatment with dose range from 0 to 10  $\mu$ M. PF-03084014 inhibited prostate cancer growth in all cell lines (Fig.1B). We next tested the expression of notch pathway activation marker notch-1 receptor intercellular domain (NICD). PF-03084014 induced a dose-dependent decrease of NICD expression in all four prostate cancer cell lines (Fig.1C). We reconfirmed that Du145R and PC3R were still resistant to docetaxel (Fig. 1D). We next evaluated the effect of PF-03084014 on responsiveness to docetaxel. PF-03084014 (10 $\mu$ M for 48hr) alone had no impact on cell viability (Fig. 1E docetaxel at 0 nM); whereas, it enhanced responsiveness to docetaxel by approximately 50% for Du145R cells and 75 to 85% for PC3R at levels of docetaxel above 10 nM (Fig. 1E). (Fig.1E). As PF-03084014 only partially sensitized the cells to docetaxel, we examined the expression of NICD in the cells that survived the docetaxel treatment in combination with PF-03084014 treatment. Both Du145R and PC3R cells were treated with PF-03084014 (10 $\mu$ M for 48hr) and either vehicle or docetaxel (50 nM) followed by immunoblot for NICD. In cells that survived docetaxel treatment in the context of Notch-1 inhibition with PF-03084014, NICD was decreased compared to the vehicle-treated cells suggesting that the resistance to docetaxel was not dependent on Notch activity in this remaining cell subpopulation (Fig. 1F). In order to provide additional

evidence that PF-03084014 mediates its effect through Notch pathway inhibition, we knocked down the Notch-1 receptor (Supplemental Fig. 1A) and evaluated its impact on basal proliferation and docetaxel sensitivity. Similar to PF-03084014, knockdown of the Notch receptor decreased cell growth and sensitized the cells to docetaxel (Supplemental Figs. 1B and 1C). Additionally, overexpression of NICD (Supplemental Fig. 1D) was able to diminish the impact of PF-03085014 on both cell growth (Supplemental Fig. 1E) and docetaxel responsiveness (Supplemental Fig. 1F). Taken together, these results indicate that PF-03085015 mediates its activity through Notch-1.

### **PF-03084014 enhances the antitumor effect of docetaxel in CRPC growing in soft tissue**

To determine if the *in vitro* impact of PF-03084014 on prostate cancer cells extended to *in vivo*, we subcutaneously injected the four cell lines into mice and treated them with vehicle, PF-03084014 alone, docetaxel alone or PF-03084014 plus docetaxel. Results are presented in Figure 2. PF-03084014 alone decreased the prostate cancer tumor volume in Du145 and PC3 by 39.7% and 28.9%, respectively; 5mg/kg docetaxel alone inhibited tumor growth in Du145 and PC3 by 36.1%, and 38.5%, respectively; the combination of the two agents increased the anti-tumor efficacy compared to either agent alone with Du145 and PC-3, decreased by 64.1% and 56.6%, respectively, which represents an additive effect. We next tested the effect of these drugs on the docetaxel-resistant cell lines; however, we used a higher dose (10mg/kg) of docetaxel than used for the docetaxel-sensitive lines (5mg/kg). The rationale for using a higher dose in the resistant cell lines was so that we could demonstrate some efficacy with docetaxel alone which would allow us to determine if PF-03084014 had a synergistic effect with the docetaxel. This still allowed us to explore if PF-03084014 sensitized the cells to docetaxel, but does not allow us to clearly determine if it sensitizes the resistant cells to the level of the sensitive cells. PF-03084014 alone decreased Du145R and PC3R by 45% and 35%, respectively. Docetaxel alone decreased Du145R and PC3R by 36% and 18%, respectively. The combination of both agents increased the anti-tumor efficacy compared to either agent alone for the PC3R and Du145R cells (74.4%, 56.7%, respectively). Overall, the effects of the combined therapies was additive and not synergistic. Mouse body weights were not impacted by treatment (data not shown) consistent with previous reports of the minimal toxicity of PF-03084014 using this dosage regimen in murine models (15, 24).

### **PF-03084014 induces a combination of decreasing proliferation, inducing apoptosis and blocking tumor angiogenesis *in vivo***

To explore cellular mechanisms that could account for the anti-tumor effects we initially assessed for tumor proliferation using Ki67 expression; apoptosis using cleaved-caspase 3 expression and vascularity using CD31 to identify microvessels. PF-03084014 alone decreased Ki67 by 42.5%, increased cleaved-caspase 3 by 91% and decreased microvessel density by 84.4% in the Du145 xenografts (Fig. 3). The combination reduced Ki67 expression by 68.3% and microvessel density by 88.4%; whereas, it increased cleaved-caspase 3 expression by 290.6%. PF-03084014 and docetaxel (at 10 mg/kg) had a similar effect on the Du145R cells (Supplemental Fig. 2). These results indicate the combination had a greater impact on all these parameters than either agent alone, albeit in an additive as opposed to synergistic fashion. Furthermore, these findings suggest that PF-03084014

inhibited tumor growth through a combination of decreasing proliferation, inducing apoptosis and blocking tumor angiogenesis.

### **PF-03084014 impairs Notch pathway and modulates other multiple pathways in docetaxel sensitive and resistant CRPC**

As PF-03084014 is designed to target  $\gamma$ -secretase, we examined Notch pathway activation, including expression of NICD and the Notch pathway target genes HEY1 and HEY2, in the subcutaneous tumor tissues. PF-03084014 alone suppressed NICD-1 expression in Du145 and Du145R cells (Supplemental Fig. 3A). PF-03084014 also decreased HEY1 and HEY2 mRNA expression in both Du145 and Du145R tumor tissues compared to vehicle (Supplemental Fig. 3B and C).

The Notch pathway crosstalks with many other signaling pathways. Accordingly, we examined related proteins in pathways that interact with Notch signaling. PF-03084014 treatment decreased the cell cycle promoting protein Cyclin E in both Du145 and Du145R cells with/without the presence of docetaxel. PF-03084014 had a global effect on expression of the apoptotic pathway BCL-2 protein family. Generally, pro-apoptotic proteins, BAK and BAX were elevated, and anti-apoptotic proteins, BCL-XL and BCL-2 were decreased (Fig. 4A). MEK-ERK pathway and PI3K-AKT impact multiple aspects of prostate cancer biology (25). PF-03084014 impaired MEK and ERK phosphorylation. Phosphorylation of AKT was inhibited in Du145 cells and PI3K phosphorylation was decreased in Du145R cells (Fig. 4B). To provide some clues as to the ability of PF-03084014 to enhance docetaxel efficacy, we examined proteins associated with epithelial-mesenchymal transition (EMT) and drug efflux proteins (Fig. 4C). PF-03084014 treatment increased E-cadherin expression, decreased vimentin expression and EMT transcription factors: snail, slug suggesting an overall inhibition of EMT. PF-03084014 treatment decreased MDR1 expression, which would suggest decreased ability of the prostate cancer cells to actively efflux drugs. EGFR was decreased in both cell lines after PF-03084014 treatment. The NF $\kappa$ B-family protein P52 was also decreased by PF-03084014 treatment (Fig. 4D).

### **PF-03084014 targets the prostate cancer stem cell**

Cancer stem cells are considered linked to elevated Notch pathway signal (26). In prostate cancer, ALDH has been suggested to serve as a biomarker of stemness (27). To examine the effect of PF-03084014 on cancer stem cells, we measured the effect of PF-03084014 on the percentage of ALDH<sup>high</sup> cells in the four groups. PF-03084014 treatment decreased the proportion of ALDH<sup>high</sup> cells compared to vehicle-treated cells in all cell lines (Fig. 5A and B). In contrast, docetaxel alone increased the percentage of ALDH<sup>high</sup> cells; however, this effect was partly blocked by PF-03084014. Consistent with the ALDH<sup>high</sup> cell results, the stem cell transcription factor nanog was decreased after PF-03084014 treatment, but increased by docetaxel alone and decreased by the combination of both (Fig. 5C). As an indication of cancer stem cell function, we evaluate the impact of treatments on prostasphere formation. PF-03084014 resulted in decreased prostasphere formation compared to docetaxel treatment alone, which increased prostasphere formation (Fig. 5D and 5E). In contrast, the addition of PF-03084014 inhibited the docetaxel-induced increase of prostaspheres. To determine if the *in vitro* cancer stem cells result translated to tumor

recurrence, after 4 weeks of treatment in the Du145 cell group, we stopped treatment to allow for tumor regrowth. The tumors in the mice that had been treated with the combination of PF-03084014 and docetaxel grew slower with a longer tumor doubling time than those treated with docetaxel alone (37.07 days vs. 15.54 days) (Fig.5F). Taken together, these results suggest that PF-03084014 targets cancer stem cells which contributes to delayed tumor regrowth.

### **PF-03084014 treatment leads to the reversal of docetaxel resistance in bone**

As CRPC progresses, the majority of men develop bone metastases (2). Thus, we evaluated if the antitumor effects of PF-03084014 observed in soft tissues extended to prostate cancer growing in bone. Du145R cells were injected into the tibiae of mice and tumors were allowed to develop over 8 weeks at which time they were treated with vehicle, PF-03084014 alone, docetaxel alone or the combination of PF-03084014 and docetaxel. While PF-03084014 alone inhibited the tumor growth, docetaxel alone did not (Fig. 6A). However, the combination of PF-03084014 and docetaxel induced a markedly increased tumor response than either drug alone. To assess for impact of treatment on proliferation, tumor tissues were stained for Ki67. PF-03084014 induced a 19.8% reduction in Ki67 positivity compared to vehicle-treated mice; while docetaxel alone had no effect; however, the combination of both drugs reduced Ki67 by 48% (Fig. 6B). To assess for impact of treatment on apoptosis, tissues were subjected to Apoptag. PF-03084014 induced an increase in Apoptag staining of 1.9-fold and the combination of both PF-03084014 and docetaxel increased Apoptag staining by 6.7-fold (Fig. 6B). These results indicate that the PF-03084014 can enhance docetaxel-mediated cytotoxicity in docetaxel resistant cells growing in bone through a combination of inhibiting proliferation and promoting apoptosis.

## **Discussion**

In this study, we demonstrated that using a GSI to target Notch signaling has both single-agent anti-tumor effects as well as adjunct activity with docetaxel-mediated cytotoxicity on prostate cancer. We further determined that GSI-mediated anti-tumor activity was associated with both inhibition of proliferation and promotion of apoptosis. Furthermore, the GSI resulted in impacting multiple different tumor promoting pathways and decreased cancer stem cell activity. These results provide both (1) evidence that inhibition of Notch signaling may have therapeutic benefit for prostate cancer patients through enhancing efficacy of docetaxel and (2) potential cellular and molecular mechanisms as to how inhibition of Notch mediates its anti-tumor activity in prostate cancer.

A unique characteristic of the Notch pathway is that the ligands (Jagged-1,2 and Delta-1,3,4) and receptors (Notch-1,2,3,4) are both type I membrane proteins. After cell-cell direct contact, notch receptors are cleaved by  $\gamma$ -secretase, releasing an intracellular domain (NICD) that translocates into the nucleus to modulate transcription (26). As the Notch pathway is considered to be important in cell-fate determination, it is not surprising that it is induced during prostate growth in the embryo. However, the role of Notch in prostate cancer is controversial and not well-defined (28). Both knockout and overexpression of Notch-1 demonstrated anti-proliferative effects in prostate cancer (9). In clinical prostate cancer



tissues, upregulation of Notch pathway components has been observed (29) suggesting it may play a role in prostate cancer. This latter observation is consistent with our results which demonstrate for the first time that using a GSI for pharmacological inhibition of the Notch pathway may have an anti-tumor effect and enhance docetaxel-mediated cytotoxicity for prostate cancer. Our results are consistent with previous publications that Notch inhibition can impact several non-prostate solid tumors (16-18) and build on the previous report that genetic inhibition of Notch can reverse docetaxel sensitivity (14). However, our observation that the cells that maintained resistance to the combination of PF-03084014 and docetaxel had low levels of NICD, indicated that additional signaling pathways contribute to chemoresistance, such as previously shown for Notch and Hedgehog in combination (14).

Tumor growth is composed of a balance between cell proliferation and cell apoptosis. These activities are regulated by many factors such as cyclin proteins, the BCL-2 family, MEK-ERK, PI3K-AKT pathway etc (30). Also, EGFR and NF- $\kappa$ B pathways contribute to the prostate cancer cell growth (31, 32). It is well known Notch pathway interacts with many different signaling cascades to regulate critical cellular processes (26). In different cancers, the inhibition of Notch-1 has been reported to induce G2/M cell cycle arrest (33), upregulate apoptosis via anti-BCL-XL, BCL-2 (34, 35), and impair phosphorylation of MEK (36) and AKT (37). Our results reflect that GSI treatment of prostate cancer involves many of these activities and thus suggest that the anti-tumor effects of Notch inhibition in prostate cancer involves multiple mechanisms that culminate in an overall inhibition of tumor growth through both inhibition of proliferation and induction of apoptosis.

The addition of PF-03084014 to docetaxel resulted in enhanced docetaxel-mediated anti-tumor activity, even in the context of docetaxel resistant cells. Docetaxel mediates its antitumor activity through two key mechanisms: (1) inhibition of microtubular depolymerization and (2) attenuation of the anti-apoptotic activity of BCL-2 and BCL-XL (38). Docetaxel-mediated inhibition of microtubular depolymerization induces cell cycle arrest at G2/M; whereas, inhibition of the Notch pathway results in G1/S arrest via decreased Cyclin E expression (39). This suggests that combination of two agents may complement each other to result in enhanced arrest. In terms of impacting apoptosis, docetaxel inhibits anti-apoptotic BCL-2 activity, PF-03084014 also down-regulated the expression, so the combination induced more than either single-agent alone. Third, docetaxel promotes Notch pathway activity as demonstrated by the increase of NICD1. This may result in diminishing docetaxel's cytotoxic activity, through promotion of Notch activity. Thus the ability of PF-03084014 to inhibit this effect results in enhancing docetaxel-mediated killing.

The treatment of CRPC, especially docetaxel-resistant CRPC remains a therapeutic challenge. Our observation that PF-03084014 delayed growth of docetaxel-resistant CRPC cells in both soft tissue and bone environments provides the suggestion that targeting Notch may enhance therapy of CRPC. Moreover, its efficacy in restoring docetaxel-sensitivity to docetaxel-resistant cells suggests it would be useful in an adjuvant setting. Multiple mechanisms have been suggested to contribute to the development of docetaxel resistance (40). PF-03084014 impacted many of these mechanisms in the docetaxel-resistant cells including altering BCL-2 family member activity, impairing proliferative signaling (cyclin

E, MEK-ERK and PI3K-AKT), inhibiting oncogenic protein expression (EGFR and P52) and inhibiting MDR-1 expression. Furthermore, epithelial mesenchymal transition (EMT) has been associated with induction of docetaxel resistance (40). Notch may contribute to this through mediating TGF-beta1-induced EMT through the induction of Snail1 (41). Thus, PF-03084014, which inhibits Notch activity, may improve docetaxel-responsiveness through multiple mechanisms.

The Notch pathway has been reported to contribute to cancer stem cell biology in many different cancers (42-44). In prostate cancer, stem-like CD133<sup>high</sup>/CD44<sup>high</sup> Du145 cells showed elevated expression of multiple Notch pathway genes (45). This led us to examine GSI-mediated alteration of cancer stem cells in the prostate cancer models. Our observation that docetaxel alone resulted in an increased proportion of cancer stem cells in remaining tumor is consistent with the chemoresistant nature of cancer stem cells and the propensity for tumor to reoccur. In contrast, PF-03084014 decreased the proportion of cancer stem cells, thus countering the effect of docetaxel resulting in enhanced and longer duration of therapeutic effect.

Tumor-induced angiogenesis is a major contributor to tumor growth (46). The Notch pathway has been shown to promote angiogenesis of many solid tumors, including breast cancer (47) and pancreatic cancer (17). Although not clearly demonstrated, Notch signaling is likely involved in prostate cancer-associated angiogenesis (48). Our observation that PF-03084014 reduced microvessel density supports this possibility. Although not evaluated in the current study, Notch signaling in breast cancer has been shown to promote angiogenesis through VEGF/VEGFR2 activity (47). One mechanism through which PF-03084014 may have inhibited angiogenesis was through decreased NF-κB signaling (based on our observation of decreased p52) which is known to contribute to angiogenesis (32). Regardless of the mechanism, the ability of PF-03084014 to decrease microvessel density suggests another mechanism through which this GSI contributes to an anti-cancer effect.

This experiment has several limitations. We used subcutaneous not orthotopic injection to model soft tissue growth. Although orthotopic injection is ideal, it is challenging to model as mice have four biologically different and anatomically separated lobes of the prostate and it is not clearly defined how well any of them recapitulate the human prostate. Another limitation to these studies is that the cell lines used were androgen receptor negative. As androgen receptor signaling is an important component of prostate cancer, even in some cases of CRPC, our studies did not totally recapitulate the clinical disease.

In summary, this research identified that inhibition of Notch signaling using PF-03084014 had an antitumor effect in a murine model of CRPC. Furthermore, PF-03084014 had adjuvant activity with docetaxel and importantly enhanced docetaxel-mediated cytotoxicity on docetaxel-resistant cells. These findings suggest that GSIs, such as PF-03084014, should be evaluated in clinical trials as adjuvants to docetaxel for therapy of CRPC and docetaxel-resistant prostate cancer.

## Supplementary Material

Refer to Web version on PubMed Central for supplementary material.

## References

1. Siegel R, Naishadham D, Jemal A. Cancer statistics, 2013. *CA Cancer J Clin.* 2013; 63:11–30. [PubMed: 23335087]
2. Cookson MS, Roth BJ, Dahm P, Engstrom C, Freedland SJ, Hussain M, et al. Castration-resistant prostate cancer: AUA Guideline. *J Urol.* 2013; 190:429–38. [PubMed: 23665272]
3. Tannock IF, de Wit R, Berry WR, Horti J, Pluzanska A, Chi KN, et al. Docetaxel plus prednisone or mitoxantrone plus prednisone for advanced prostate cancer. *N Engl J Med.* 2004; 351:1502–12. [PubMed: 15470213]
4. Francini E, Petrioli R, Rossi G, Laera L, Roviello G. PSA response rate as a surrogate marker for median overall survival in docetaxel-based first-line treatments for patients with metastatic castration-resistant prostate cancer: an analysis of 22 trials. *Tumour Biol.* 2014
5. Beltran H, Beer TM, Carducci MA, de Bono J, Gleave M, Hussain M, et al. New therapies for castration-resistant prostate cancer: efficacy and safety. *Eur Urol.* 2011; 60:279–90. [PubMed: 21592649]
6. Guruharsha KG, Kankel MW, Artavanis-Tsakonas S. The Notch signalling system: recent insights into the complexity of a conserved pathway. *Nat Rev Genet.* 2012; 13:654–66. [PubMed: 22868267]
7. Andersson ER, Sandberg R, Lendahl U. Notch signaling: simplicity in design, versatility in function. *Development.* 2011; 138:3593–612. [PubMed: 21828089]
8. Villaronga MA, Bevan CL, Belandia B. Notch signaling: a potential therapeutic target in prostate cancer. *Curr Cancer Drug Targets.* 2008; 8:566–80. [PubMed: 18991567]
9. Leong KG, Gao W-Q. The Notch pathway in prostate development and cancer. *Differentiation.* 2008; 76:699–716. [PubMed: 18565101]
10. Ross AE, Marchionni L, Vuica-Ross M, Cheadle C, Fan J, Berman DM, et al. Gene expression pathways of high grade localized prostate cancer. *Prostate.* 2011
11. Zhang Y, Wang Z, Ahmed F, Banerjee S, Li Y, Sarkar FH. Down-regulation of Jagged-1 induces cell growth inhibition and S phase arrest in prostate cancer cells. *Int J Cancer.* 2006; 119:2071–7. [PubMed: 16823852]
12. Bin Hafeez B, Adhami VM, Asim M, Siddiqui IA, Bhat KM, Zhong W, et al. Targeted knockdown of Notch1 inhibits invasion of human prostate cancer cells concomitant with inhibition of matrix metalloproteinase-9 and urokinase plasminogen activator. *Clin Cancer Res.* 2009; 15:452–9. [PubMed: 19147749]
13. Wang Z, Li Y, Banerjee S, Kong D, Ahmad A, Nogueira V, et al. Down-regulation of Notch-1 and Jagged-1 inhibits prostate cancer cell growth, migration and invasion, and induces apoptosis via inactivation of Akt, mTOR, and NF-kappaB signaling pathways. *J Cell Biochem.* 2010; 109:726–36. [PubMed: 20052673]
14. Domingo-Domenech J, Vidal SJ, Rodriguez-Bravo V, Castillo-Martin M, Quinn SA, Rodriguez-Barrueco R, et al. Suppression of acquired docetaxel resistance in prostate cancer through depletion of notch- and hedgehog-dependent tumor-initiating cells. *Cancer Cell.* 2012; 22:373–88. [PubMed: 22975379]
15. Wei P, Walls M, Qiu M, Ding R, Denlinger RH, Wong A, et al. Evaluation of selective gamma-secretase inhibitor PF-03084014 for its antitumor efficacy and gastrointestinal safety to guide optimal clinical trial design. *Mol Cancer Ther.* 2010; 9:1618–28. [PubMed: 20530712]
16. Zhang CC, Yan Z, Zong Q, Fang DD, Painter C, Zhang Q, et al. Synergistic effect of the gamma-secretase inhibitor PF-03084014 and docetaxel in breast cancer models. *Stem Cells Transl Med.* 2013; 2:233–42. [PubMed: 23408105]
17. Yabuuchi S, Pai SG, Campbell NR, de Wilde RF, De Oliveira E, Korangath P, et al. Notch signaling pathway targeted therapy suppresses tumor progression and metastatic spread in pancreatic cancer. *Cancer Lett.* 2013; 335:41–51. [PubMed: 23402814]

18. Arcaroli JJ, Quackenbush KS, Purkey A, Powell RW, Pitts TM, Bagby S, et al. Tumours with elevated levels of the Notch and Wnt pathways exhibit efficacy to PF-03084014, a gamma-secretase inhibitor, in a preclinical colorectal explant model. *Br J Cancer*. 2013; 109:667–75. [PubMed: 23868008]
19. Takeda M, Mizokami A, Mamiya K, Li YQ, Zhang J, Keller ET, et al. The establishment of two paclitaxel-resistant prostate cancer cell lines and the mechanisms of paclitaxel resistance with two cell lines. *Prostate*. 2007; 67:955–67. [PubMed: 17440963]
20. Wang Z, Zhang Y, Li Y, Banerjee S, Liao J, Sarkar FH. Down-regulation of Notch-1 contributes to cell growth inhibition and apoptosis in pancreatic cancer cells. *Mol Cancer Ther*. 2006; 5:483–93. [PubMed: 16546962]
21. Sottnik JL, Campbell B, Mehra R, Behbahani-Nejad O, Hall CL, Keller ET. Osteocytes serve as a progenitor cell of osteosarcoma. *J Cell Biochem*. 2014; 115:1420–9. [PubMed: 24700678]
22. Jiang Y, Dai J, Zhang H, Sottnik JL, Keller JM, Escott KJ, et al. Activation of the Wnt pathway through AR79, a GSK3beta inhibitor, promotes prostate cancer growth in soft tissue and bone. *Mol Cancer Res*. 2013; 11:1597–610. [PubMed: 24088787]
23. Li J-L, Sainson RCA, Shi W, Leek R, Harrington LS, Preusser M, et al. Delta-like 4 Notch ligand regulates tumor angiogenesis, improves tumor vascular function, and promotes tumor growth in vivo. *Cancer Res*. 2007; 67:11244–53. [PubMed: 18056450]
24. Lanz TA, Wood KM, Richter KE, Nolan CE, Becker SL, Pozdnyakov N, et al. Pharmacodynamics and pharmacokinetics of the gamma-secretase inhibitor PF-3084014. *J Pharmacol Exp Ther*. 2010; 334:269–77. [PubMed: 20363853]
25. Georgi B, Korzeniewski N, Hadaschik B, Grüllich C, Roth W, Sülmann H, et al. Evolving therapeutic concepts in prostate cancer based on genome-wide analyses (review). *Int J Oncol*. 2014; 45:1337–44. [PubMed: 25070358]
26. Miele L. Notch signaling. *Clin Cancer Res*. 2006; 12:1074–9. [PubMed: 16489059]
27. Hellsten R, Johansson M, Dahlman A, Sterner O, Bjartell A. Galiellalactone inhibits stem cell-like ALDH-positive prostate cancer cells. *PLoS One*. 2011; 6:e22118. [PubMed: 21779382]
28. Carvalho FLF, Simons BW, Eberhart CG, Berman DM. Notch signaling in prostate cancer: a moving target. *Prostate*. 2014; 74:933–45. [PubMed: 24737393]
29. Shou J, Ross S, Koeppen H, de Sauvage FJ, Gao WQ. Dynamics of notch expression during murine prostate development and tumorigenesis. *Cancer Res*. 2001; 61:7291–7. [PubMed: 11585768]
30. McCubrey JA, Steelman LS, Chappell WH, Abrams SL, Wong EWT, Chang F, et al. Roles of the Raf/MEK/ERK pathway in cell growth, malignant transformation and drug resistance. *Biochim Biophys Acta*. 2007; 1773:1263–84. [PubMed: 17126425]
31. Traish AM, Morgentaler A. Epidermal growth factor receptor expression escapes androgen regulation in prostate cancer: a potential molecular switch for tumour growth. *Br J Cancer*. 2009; 101:1949–56. [PubMed: 19888222]
32. Suh J, Rabson AB. NF-kappaB activation in human prostate cancer: important mediator or epiphenomenon? *J Cell Biochem*. 2004; 91:100–17. [PubMed: 14689584]
33. Wu K, Zhang L, Lin Y, Yang K, Cheng Y. Inhibition of gamma-secretase induces G2/M arrest and triggers apoptosis in renal cell carcinoma. *Oncol Lett*. 2014; 8:55–61. [PubMed: 24959218]
34. Timme CR, Gruidl M, Yeatman TJ. Gamma-secretase inhibition attenuates oxaliplatin-induced apoptosis through increased Mcl-1 and/or Bcl-xL in human colon cancer cells. *Apoptosis*. 2013; 18:1163–74. [PubMed: 23887890]
35. Gao F, Yao M, Shi Y, Hao J, Ren Y, Liu Q, et al. Notch pathway is involved in high glucose-induced apoptosis in podocytes via Bcl-2 and p53 pathways. *J Cell Biochem*. 2013; 114:1029–38. [PubMed: 23129176]
36. Li JY, Li RJ, Wang HD. gamma-secretase inhibitor DAPT sensitizes t-AUCB-induced apoptosis of human glioblastoma cells in vitro via blocking the p38 MAPK/MAPKAP2/Hsp27 pathway. *Acta Pharmacol Sin*. 2014; 35:825–31. [PubMed: 24793313]
37. Sangphech N, Osborne BA, Palaga T. Notch signaling regulates the phosphorylation of Akt and survival of lipopolysaccharide-activated macrophages via regulator of G protein signaling 19 (RGS19). *Immunobiology*. 2014; 219:653–60. [PubMed: 24775271]

38. Pienta KJ. Preclinical mechanisms of action of docetaxel and docetaxel combinations in prostate cancer. *Semin Oncol.* 2001; 28:3–7. [PubMed: 11685722]
39. Malumbres M, Barbacid M. Cell cycle, CDKs and cancer: a changing paradigm. *Nat Rev Cancer.* 2009; 9:153–66. [PubMed: 19238148]
40. Holohan C, Van Schaeybroeck S, Longley DB, Johnston PG. Cancer drug resistance: an evolving paradigm. *Nat Rev Cancer.* 2013; 13:714–26. [PubMed: 24060863]
41. Matsuno Y, Coelho AL, Jarai G, Westwick J, Hogaboam CM. Notch signaling mediates TGF-beta1-induced epithelial-mesenchymal transition through the induction of Snai1. *Int J Biochem Cell Biol.* 2012; 44:776–89. [PubMed: 22330899]
42. Jiang LY, Zhang XL, Du P, Zheng JH. gamma-Secretase Inhibitor, DAPT Inhibits Self-renewal and Stemness Maintenance of Ovarian Cancer Stem-like Cells In Vitro. *Chin J Cancer Res.* 2011; 23:140–6. [PubMed: 23482909]
43. Arcaroli JJ, Powell RW, Varella-Garcia M, McManus M, Tan AC, Quackenbush KS, et al. ALDH + tumor-initiating cells exhibiting gain in NOTCH1 gene copy number have enhanced regrowth sensitivity to a gamma-secretase inhibitor and irinotecan in colorectal cancer. *Mol Oncol.* 2012; 6:370–81. [PubMed: 22521243]
44. Kondratyev M, Kreso A, Hallett RM, Girgis-Gabardo A, Barcelon ME, Ilieva D, et al. Gamma-secretase inhibitors target tumor-initiating cells in a mouse model of ERBB2 breast cancer. *Oncogene.* 2012; 31:93–103. [PubMed: 21666715]
45. Oktem G, Bilir A, Uslu R, Inan SV, Demiray SB, Atmaca H, et al. Expression profiling of stem cell signaling alters with spheroid formation in CD133/CD44 prostate cancer stem cells. *Oncol Lett.* 2014; 7:2103–9. [PubMed: 24932297]
46. Hanahan D, Weinberg RA. Hallmarks of cancer: the next generation. *Cell.* 2011; 144:646–74. [PubMed: 21376230]
47. Zhou W, Wang G, Guo S. Regulation of angiogenesis via Notch signaling in breast cancer and cancer stem cells. *Biochim Biophys Acta.* 2013; 1836:304–20. [PubMed: 24183943]
48. Marignol L, Rivera-Figueroa K, Lynch T, Hollywood D. Hypoxia, notch signalling, and prostate cancer. *Nature Reviews Urology.* 2013

### Statement of Translational Relevance

Docetaxel is often used as first line therapy for castration-resistant prostate cancer (CRPC). However, only a subset of patients demonstrate a response and eventually the majority of patients develop resistance. Accordingly, identifying methods to enhance docetaxel therapy of CRPC would provide significant clinical gains for patients. In the current report, we identified that inhibition of Notch signaling using PF-03084014, a  $\gamma$ -secretase inhibitor (GSI), enhanced docetaxel-mediated cytotoxicity on docetaxel-resistant cells *in vitro* and *in vivo*. PF-03084014 achieved this activity through inhibiting cancer cell proliferation, angiogenesis and cancer stem cell sequestration and through promoting cancer cell apoptosis. These findings suggest that GSIs, such as PF-03084014, should be evaluated in clinical trials as adjuvants to docetaxel for therapy of CRPC and docetaxel-resistant prostate cancer.

Author Manuscript

Author Manuscript

Author Manuscript

Author Manuscript

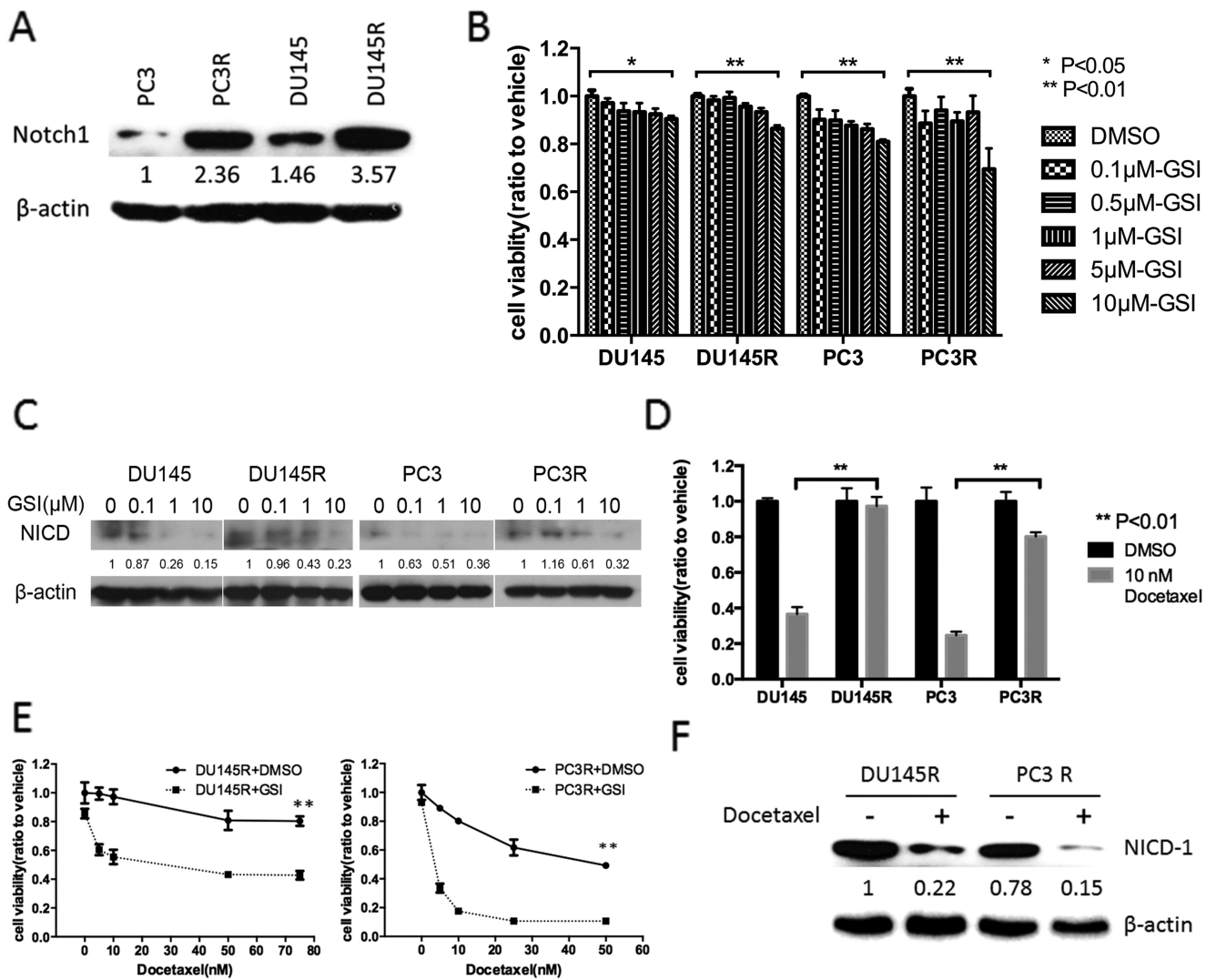


**Figure 1. PF-03084014 sensitizes docetaxel-resistant cells to docetaxel *in vitro***

(A) Total protein was isolated from the indicated prostate cancer cells and subject to immunoblot for Notch-1.  $\beta$ -actin was used as loading control. Bands were measured using densitometry and values first normalized to respective  $\beta$ -actin bands and then reported below each gel as relative to PC3. (B)  $2.5 \times 10^3$  of the indicated prostate cancer cells were treated with vehicle (DMSO) or PF-03084014 (0.1  $\mu$ M, 0.5  $\mu$ M, 1  $\mu$ M, 5  $\mu$ M, 10  $\mu$ M) for 48 hours. Cell viability was measured using resazurin cell viability assays. (C) After the treatment with vehicle (DMSO) or PF-03084014 (0.1  $\mu$ M, 1  $\mu$ M, 10  $\mu$ M) for 48 hours, protein was extracted from the prostate cancer cells and subjected to immunoblot analysis for Notch-1 receptor intercellular domain (NICD).  $\beta$ -actin was used as loading control. Bands were measured using densitometry and values first normalized to respective  $\beta$ -actin bands and then reported below each gel as relative to 0  $\mu$ M GSI. (D)  $2.5 \times 10^3$  prostate cancer cells were treated with vehicle (DMSO) or docetaxel (10  $\mu$ M) for 48 hours. Cell viability was measured using resazurin cell viability assays. (E)  $2.5 \times 10^3$  DU145R and PC3R cells were treated with docetaxel (0nM, 5nM, 10nM, 25nM, 50nM, 75nM) and PF-03084014 (10  $\mu$ M) or vehicle

(DMSO) for 48 hours. Cell viability was measured using resazurin cell viability assays. (F) Cells were treated with PF-03084014 as in (E) using 10 nM docetaxel or vehicle for 48 hours. Total protein was then isolated from remaining cells and subjected to immunoblot for NICD.  $\beta$ -actin was used as loading control. Bands were measured using densitometry and values first normalized to respective  $\beta$ -actin bands and then reported below each gel as relative to vehicle-treated Du145. \* $p < 0.05$ , \*\* $p < 0.01$ .

Author Manuscript

Author Manuscript

Author Manuscript

Author Manuscript



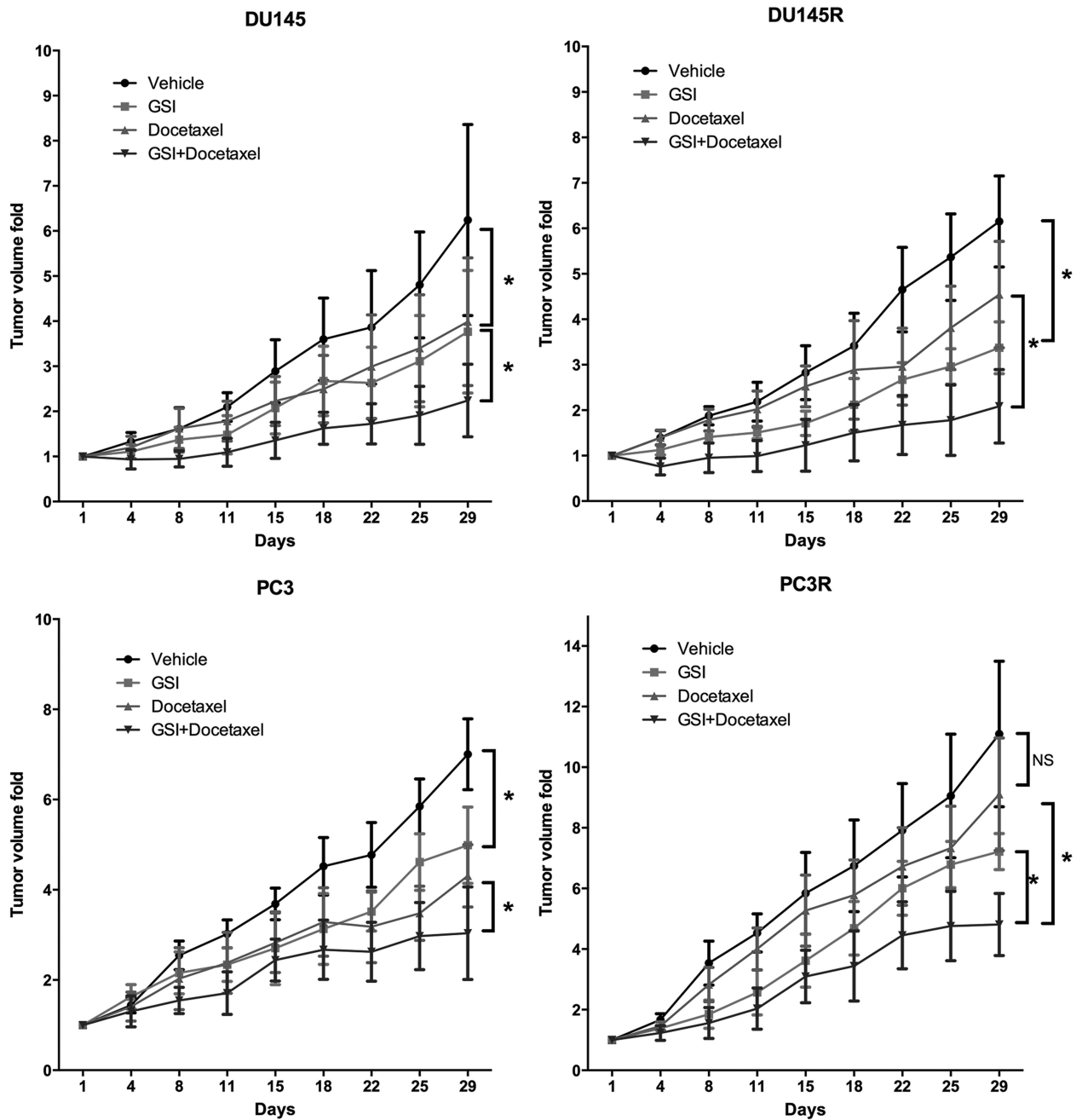


**Figure 2. The combination of PF-03084014 and docetaxel has a greater antitumor effect than either agent alone in prostate cancer growing in soft tissue**

Du145, Du145R, PC3 or PC3R cells ( $1 \times 10^6$ ) were injected subcutaneously into mice. When cohorts of tumors reached 100-200 mm<sup>3</sup>, mice were randomized and treated with vehicle, PF-03084014, docetaxel, PF-03084014+Docetaxel as described in Materials and Methods (N=7-8 mice per group). Tumors were measured using calipers biweekly until 28 days of treatment, at which time mice were euthanized. (\*p<0.05; NS=no significant difference).

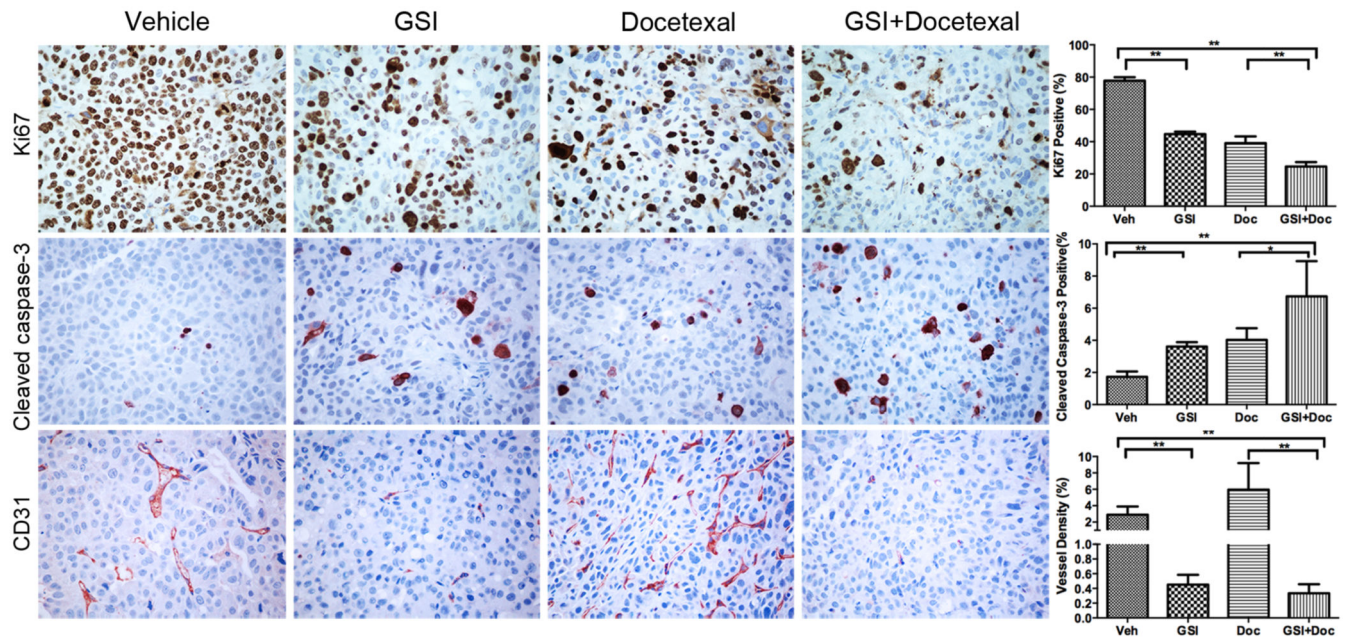


**Figure 3. PF-03084014 combined with docetaxel suppresses tumor cell proliferation, induces apoptosis and inhibits tumor angiogenesis in mice**

At end of study, tumors were harvested from the mice described in Figure 2. A portion of the Du145 tumor xenografts (n=5) were subjected to immunohistochemistry for proliferation (anti-Ki67), apoptosis (anti-cleaved Caspase 3) and tumor angiogenesis (anti-CD31). Left: Representative photomicrographs of Ki67, cleaved-caspase 3 and CD31 stained tumor sections ( $\times 40$ ). Right: Quantitation of Ki-67, cleaved-caspase 3 and CD31 positive percentage (\*  $p < 0.05$ ; \*\*  $p < 0.01$ ).

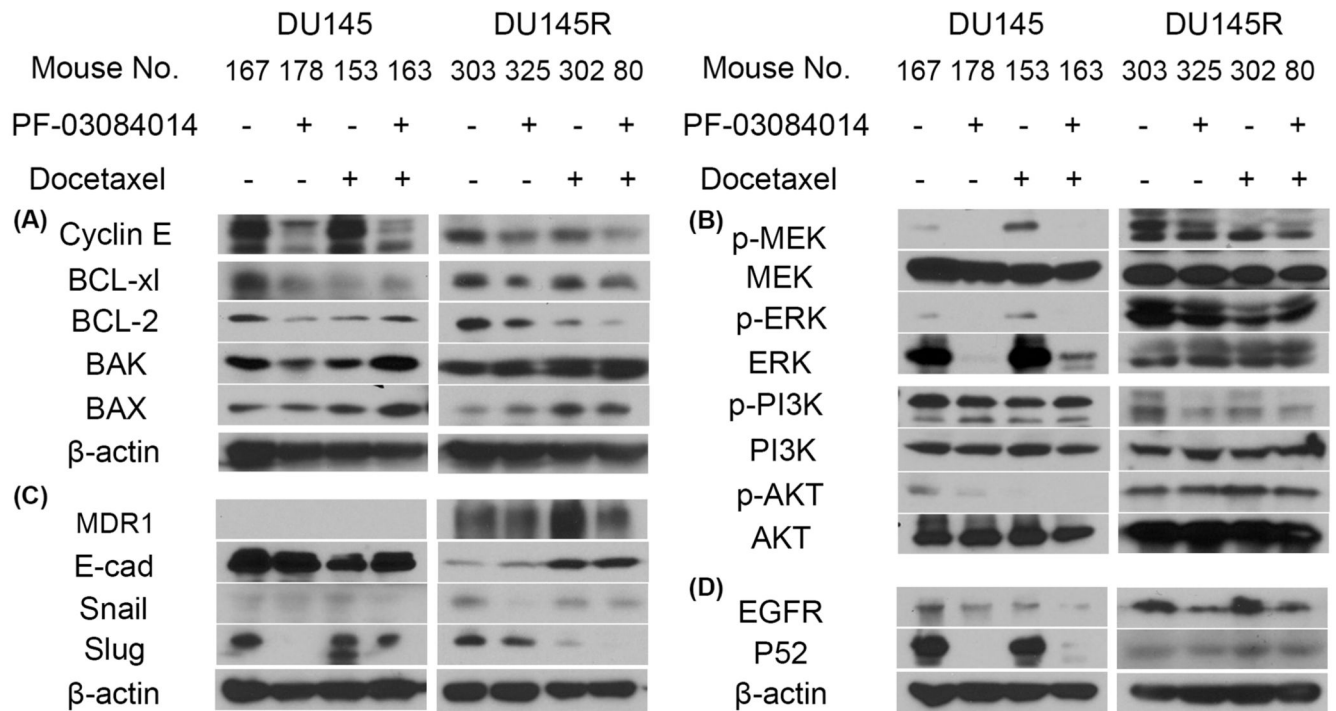


**Figure 4. PF-03084014 modulates multiple pro-tumorigenic pathways in docetaxel sensitive and resistant CRPC**

At end of study, tumors were harvested from the mice described in Figure 2. Protein and mRNA were extracted from DU145 and Du145R tumor xenografts. Proteins were subjected to immunoblot analysis for the indicated targets. (A) Cell cycle and apoptosis pathway proteins; (B) Total and phospho-proteins for several kinase pathways; (C) Epithelial to mesenchymal transition and multidrug resistance 1(MDR1) proteins; (D) EGFR and P52. Results were repeated with at least three different tumors for each treatment.

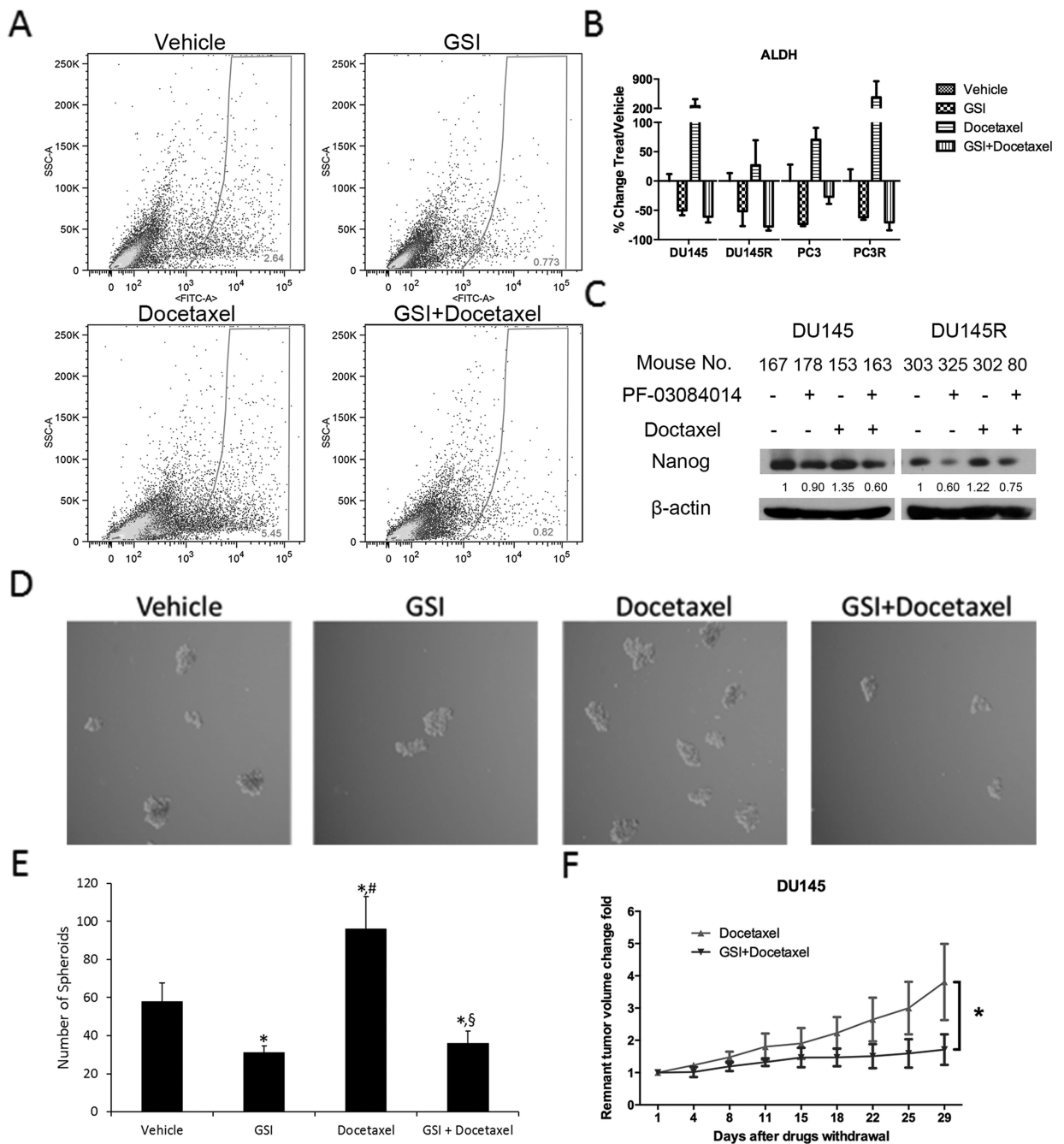


**Figure 5. PF-03084014 targets the prostate cancer stem cell**

At end of study, tumors were harvested from the mice described in Figure 2 and a portion was made into single cell suspensions. (A) Example of flow cytometry of ALDH<sup>high</sup> cells in Du145 single cell suspensions from tumor xenografts after 4 weeks treatment. Each sample was tested under identical conditions in the presence of the ALDH inhibitor diethylaminobenzaldehyde (DEAB). All gates in each sample were created using the DEAB-treated corresponding sample. (B) Quantitation of ALDH<sup>high</sup> cells percentages from the four cell lines among the different treatment groups. (C) Tumor-derived protein (as

described in Fig.4) was subjected to immunoblot analysis using anti-Nanog as primary antibody.  $\beta$ -actin was used as an internal control. Bands were measured using densitometry and values first normalized to respective  $\beta$ -actin bands and then reported below each gel as relative to the vehicle-treated mice. (D) Single cells derived from the Du145 xenografts were plated ( $1 \times 10^6$ ) in low attachment culture plates and after 7 days prostaspheres were harvested and replated ( $1 \times 10^3$ ). Du145 cells were implanted subcutaneously in mice (n=5) as and treatd as described in Figure 2. At 28 days of treatment, tumors were harvested and tested for prostasphere formation. Representative pictures of second-generation prostaspheres derived from the indicated treatments are shown. (E) The numbers of spheres formed from 1000 cells are presented (right). \* $p < 0.05$  vs. Vehicle; # $p < 0.05$  vs. GSI; § $p < 0.05$  vs. Docetaxel. (F) One set of mice (N=5/group) with Du145 xenografts treated with docetaxel alone or PF-03084014+docetaxel, as described in Figure 2, had drugs withdrawn at end of study and tumor monitoring was continued. Doubling time was calculated from the tumor growth curves; \*  $p < 0.05$ .

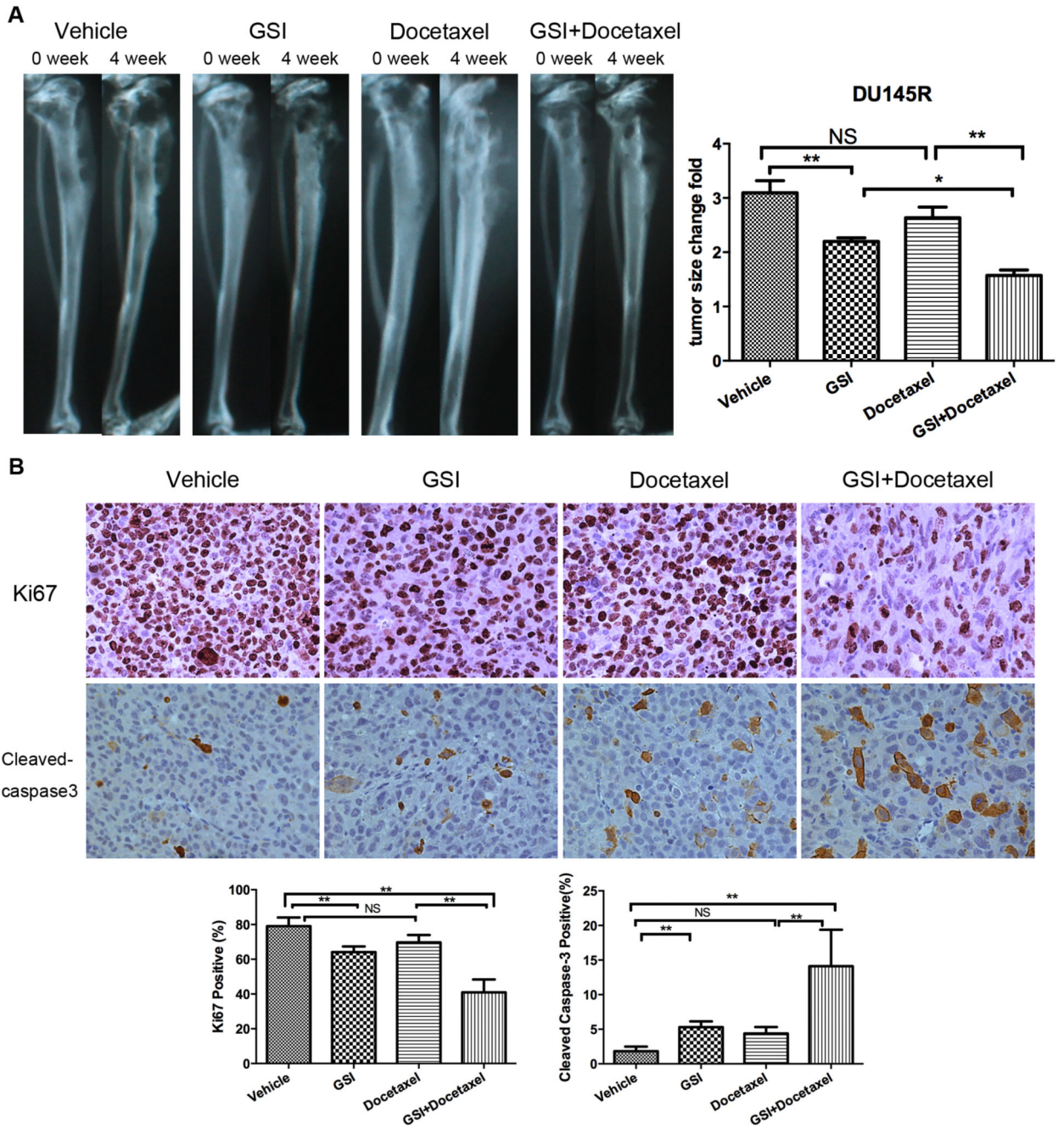


**Figure 6. The combination of PF-03084014 and docetaxel has a greater antitumor effect than either agent alone in prostate cancer growing in bone**  
 Du145R cells ( $2 \times 10^5$ ) were injected into the tibiae of mice. After eight weeks, mice were randomized and treated with vehicle, PF-03084014, docetaxel, PF-03084014+Docetaxel as described in Materials and Methods (N=5 mice per group). (A) radiographs before and after four-weeks treatment and quantitation of tumor growth based on bone changes, data represent the mean  $\pm$  SD of tumor area, \*  $p < 0.05$ ; \*\*  $p < 0.01$ , NS=no significant difference. (B) Tumor xenografts from bone were subjected to immunohistochemistry for proliferation (anti-Ki67) and apoptosis (anti-cleaved Caspase 3). Upper: Representative

photomicrographs of Ki67, cleaved-caspase 3 stained tumor sections ( $\times 40$ ). Lower: Quantitation of Ki-67 and cleaved-caspase 3 positive percentage (\*\*  $p < 0.01$ , NS=no significant difference).

Author Manuscript

Author Manuscript

Author Manuscript

Author Manuscript